**Title**
CRYOGENIC MECHANICAL PROPERTIES OF Al-Cu-Li-Zr ALLOY 2090



**Author**
Glazer, J.

**Publication Date**
1985-08-01

# Lawrence Berkeley Laboratory
UNIVERSITY OF CALIFORNIA

## Materials & Molecular Research Division



Presented at the International Cryogenic Materials Conference, Cambridge, MA, August 12-16, 1985

CRYOGENIC MECHANICAL PROPERTIES OF Al-Cu-Li-Zr ALLOY 2090

J. Glazer, S.L. Verzasconi, E.N.C. Dalder, W. Yu, R.A. Emigh, R.O. Ritchie, and J.W. Morris, Jr.

August 1985



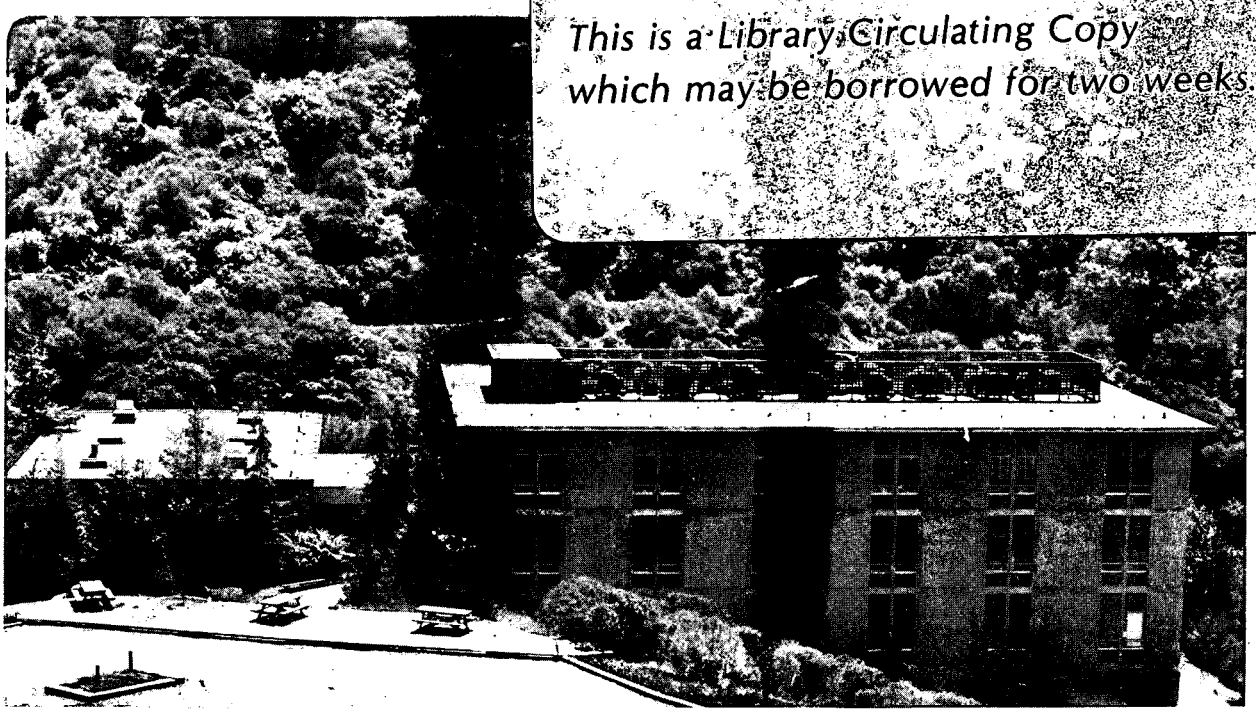

Prepared for the U.S. Department of Energy under Contract DE-AC03-76SF00098

## DISCLAIMER

# CRYOGENIC MECHANICAL PROPERTIES OF Al-Cu-Li-Zr ALLOY 2090

J. Glazer, S.L. Verzasconi, E.N.C. Dalder*, W. Yu,
R.A. Emigh, R.O. Ritchie and J.W. Morris, Jr.

Materials and Molecular Research Division,
Lawrence Berkeley Laboratory, and
Department of Materials Science and Mineral Engineering
University of California, Berkeley, California

*Lawrence Livermore National Laboratory,
University of California, Livermore, California

## ABSTRACT

The mechanical properties of aluminum-lithium alloy 2090-T8E41 were evaluated at 298 K, 77 K, and 4 K. Previously reported tensile and fracture toughness properties at room temperature were confirmed. This alloy exhibits substantially improved properties at cryogenic temperatures; the strength, elongation, fracture toughness and fatigue crack growth resistance all improve simultaneously as the testing temperature decreases. This alloy has cryogenic properties superior to those of aluminum alloys currently used for cryogenic applications.

## INTRODUCTION

The dual objectives of minimizing operating costs and maximizing performance of aircraft and aerospace systems provide a powerful incentive to reduce aircraft empty weight. Recent design studies indicate that structural weight is more effectively lowered by reducing the density of structural materials than by improving their mechanical properties.[1] This conclusion has provided the rationale for the development and application of resin composites. However, the highly anisotropic properties of composites make their application difficult, and it seems likely that at least commercial aircraft will remain primarily aluminum. As a consequence, there is a strong impetus to develop advanced high strength aluminum alloys. This challenge is responsible for a renewed interest in producing low density aluminum alloys to replace current alloys. A number of promising alloys have been developed which contain additions of lithium to reduce their density.

Intensive research and development in the last several years have led to the registration of several aluminum-lithium alloys intended to replace at lower density standard commercial aluminum alloys such as 2024, an Al-Cu-Mg-Si alloy and 7075, an Al-Zn-Mg alloy. One of the new alloys is 2090,

designed to have properties similar to those of 7075-T651. In addition to having a significantly lower density, 2090 is superior to 7075 in many respects; in fact, although low toughness has been a problem of aluminum-lithium alloys in the past, the room temperature strength-toughness relationship of 2090 is better than that of any other standard aerospace alloy.[2] (see Figure 1). It appears likely that aluminum-lithium alloys will see service within the next decade.

Although aluminum-lithium alloys have been developed with aircraft structures in mind, there are a number of potential cryogenic applications for a low density, high strength, aluminum alloy. These applications include space systems, cryogenic tankage, and high-field magnet cases. Preliminary investigations by other workers have suggested that aluminum-lithium alloys may be particularly promising cryogenic alloys because their toughness tends to improve at low temperatures.[3,4] In addition, preliminary results indicate that 2090 is sufficiently weldable for cryogenic applications.

This paper is both a characterization of the room temperature mechanical properties of this new alloy, 2090, and a study of the alloy's low temperature properties.

## EXPERIMENTAL PROCEDURE

All specimens were taken from a 12.7 mm (0.5 in) plate of 2090 supplied by the Alcoa Technical Center. The plate was received in the T8E41 condition, where E41 is a proprietary thermomechanical processing treatment. The nominal composition of 2090 is Al-2.7Cu-2.2Li-0.12Zr. Registered composition limits are given in Table 1. The actual composition of the plate is still under investigation. Chemical analysis of Al-Li alloys is hampered by a lack of standards. Several analyses were performed and although all composition determinations were within the specified composition limits, they scattered widely. The alloy is hardened in the T8 condition by a combination of the coherent ordered precipitate phases $\delta'$, $T_1'$, and $T_2'$.[5]

Elastic-plastic fracture toughness tests and tensile tests were conducted at room (298 K), liquid nitrogen (77 K), and liquid helium (4 K) temperatures. Round tensile specimens with a 2.54cm (1.0 in) gauge length were tested according to ASTM standard E8-82 in both longitudinal (L) and long-transverse (LT) orientations. The 0.2% offset yield stress, ultimate tensile strength, and total elongation were determined for pairs of specimens. Compact tension specimens were tested according to ASTM standard E813-81 in both L-T and T-L orientations to determine the crack initiation toughness, $J_{Ic}$. The measured $J_{Ic}$ data were used to calculate the plane strain fracture toughness $K_{Ic}$ values. The room temperature elastic modulus of 79 GPa was used for all calculations. Since the elastic modulus of most aluminum alloys increases with decreasing temperature,[6] the low temperature $K_{Ic}$ values represent a lower limit on the actual $K_{Ic}$ values. Fracture modes were characterized using a scanning electron microscope.

Constant amplitude fatigue crack growth rate behavior of 2090 was determined over a range of $\Delta K$ values using manual load shedding techniques on 6.4 mm thick single-edge-notched four point bend specimens. Tests were conducted at room temperature in room air (relative humidity, 25%) and at

77 K (submerged in liquid nitrogen) at a load ratio $R=K_{min}/K_{max}$ of 0.1. The test frequency was 50 Hz at fatigue crack propagation rates below $10^{-5}$ mm/cycle and 20 Hz at higher crack growth rates. Crack growth was monitored using DC electrical potential methods. The fatigue threshold was defined as the value of $\Delta K$ at which the fatigue crack growth rate decreased below $10^{-8}$ mm/cycle.

Specimens for metallography were polished to 0.05 μm and then etched with Keller's etch--2.5% $HNO_3$, 1.5% HCl, 0.5% HF, balance $H_2O$--for 15 to 30 seconds. The grain structure of the 12.7 mm plate of 2090 is shown in Figure 2. Large constituent particles were not observed.

## RESULTS AND DISCUSSION

The tensile and fracture toughness properties of 2090-T8 are shown in Table 2. The data are displayed graphically in Figure 3. The room temperature data differ only slightly from those published by Alcoa.[2] Significantly, strength, elongation and toughness in both orientations increase simultaneously with decreasing temperature. The data are compared to the properties of standard aluminum alloys at room temperature in Figure 4.

The yield strength increases with decreasing temperature in both the L and LT directions. The yield strengths are identical in the two orientations at room temperature; however, at lower temperatures the strength is higher in the LT direction. The increase in yield strength is fairly typical of precipitation hardened aluminum alloys.

The fracture toughness in the L-T orientation is consistently higher than in the T-L direction. Similarly, the tensile elongation in the LT direction is considerably lower than in the L direction. Although a small difference in properties parallel to and perpendicular to the rolling direction is not unusual, the separation seen here is atypical.

It might be expected that the large increase in fracture toughness at low temperatures would be reflected in the observed fracture mode. However, the $J_{Ic}$ fracture surfaces at all three test temperatures are strikingly similar. The fracture mode at all temperatures in the L-T orientation is illustrated in Figure 5. It appears to be controlled by intergranular delamination that is linked by regions of transgranular shear. The fracture mode in the T-L orientation appears to be similar mechanistically and also does not display an obvious change with test temperature. The large amount of intergranular cracking observed in this alloy suggests that its short-transverse properties may be poor; however, the small thickness of the plate precluded any testing in the short-transverse direction.

Fatigue crack growth rate data for 2090-T8 at room temperature and at 77 K are presented in Figure 6. Similar data for 7475-T651 taken from reference 10 are included for comparison. The 123 K data shown for 7475-T651 are probably quite similar to the 77 K data, which were not measured. As can be seen in the figure, 7475 and 2090 have comparable fatigue thresholds in both temperature regimes. However, fatigue crack growth rates for 2090 are considerably lower at higher values of $\Delta K$. This difference is most pronounced at low temperatures above $\Delta K \sim 8 MPa\sqrt{m}$ where crack growth rates are extremely rapid for 7475.

Figure 7 is a comparison of the appearance of the fatigue fracture surface in the near-threshold regime at 298 K and 77 K. The room temperature fatigue surface appears to be relatively similar to those observed in other aluminum-lithium alloys; relatively brittle, crystallographic crack growth features are observed. The 77 K fatigue crack surface contains unusual ductile regions. The crack path is highly irregular and branched, a typical morphology in aluminum-lithium alloys.[11,12]

Many aluminum alloys have improved strength-toughness relationships at low temperatures. The reasons behind this phenomenon are not understood. The much greater improvement in yield strength and fracture toughness observed here is consistent with data obtained by Webster on binary Al-Li alloys[3] and on the Al-Li-Cu-Mg alloy 8090,[4] but is also unexplained. The properties of 2090-T8E41 are compared in Table 3 with those of 2219-T87, a standard high-strength cryogenic alloy. The 77 K and 4 K properties of 2090-T8 appear to surpass those of any currently available aluminum alloy.

## CONCLUSIONS

Alloy 2090-T8E41 has a better combination of strength and toughness at room temperature than the standard aerospace alloys. Its cryogenic mechanical properties - strength, elongation, fracture toughness, and fatigue crack growth resistance - all improve dramatically with decreasing temperature. The mechanism behind these improvements is not well understood at this time. The cryogenic properties of 2090 appear to be superior to existing high-strength cryogenic aluminum alloys.

## ACKNOWLEDGEMENT

The authors would like to thank the Alcoa Technical Center for supplying the material used in these experiments. The authors are also grateful to R.R. Sawtell, P.E. Bretz and R.J. Rioja, Alcoa Technical Center, for helpful discussions. This work was supported by the Director, Office of Basic Energy Sciences, Materials Science Division of the U.S. Department of Energy under Contract No. DE-AC03-76SF00098 with the Lawrence Berkeley Laboratory. It was also supported by the U.S. Department of Energy under Contract No. W-7405-ENG-48 with Lawrence Livermore National Laboratory. One of the authors, J.G., was supported by an ATT Bell Laboratories scholarship.

## REFERENCES

1. W.E. Quist, G.H. Narayanan and A.L. Wingert, Aluminum-lithium alloys for aircraft structure - overview, in: "Aluminum-Lithium Alloys II," T.H. Sanders, Jr. and E.A. Starke, Jr., eds., AIME, Warrendale, Pennsylvania, (1981), 313.
2. R.R. Sawtell, P.E. Bretz, J.I. Petit and A.K. Vasudévan, Low density aluminum alloy development, "Proceedings of 1984 SAE/Aerospace Congress and Exposition," Long Beach, California, Oct. 15-18, 1984, in press.
3. D. Webster, Aluminum-lithium alloys, Met. Prog. 125:33 (1984).
4. D. Webster, Temperature dependence of toughness in various Al-Li alloys, in: "Proceedings of the 3rd International Aluminium-Lithium Conference," Oxford, England, July, 1985, Pergamon Press,

in press.

5. R.J. Rioja and E.A. Ludwiczak, Identification of metastable phases in an Al-Cu-Li-Zr alloy (2090), in: "Proceedings of the 3rd International Aluminium-Lithium Conference, Oxford, England, July, 1985, Pergamon Press, in press.
6. J.G. Kaufman and E.W. Johnson, New data on aluminum alloys for cryogenic applications, in: "Advances in Cryogenic Engineering," vol. 6, Plenum Press, New York, (1960), 637.
7. J.G. Kaufman, F.G. Nelson, and E.W. Johnson, The properties of aluminum alloy 2219 sheet, plate, and welded joints at low tempera tures, in: "Advances in Cryogenic Engineering," vol. 8, Plenum Press, New York, (1963) 661.
8. J.G. Kaufman and M. Holt, Evaluation of fracture characteristics of aluminum alloys at cryogenic temperatures, in: "Advances in Cryogenic Engineering," vol. 10, Plenum Press, New York (1965), 77.
9. C. Fiftal, NBS/DOE Report on Cryogenic Structural Materials for Superconducting Magnets, Vol. 1, 1978.
10. W. Yu, Thermally activated processes associated with fatigue thresholds in Fe-Si binary and aluminum alloys, PhD thesis, University of Minnesota (1983).
11. S. Suresh and A.K. Vasudévan, Influence of composition and microstructure on constant and variable amplitude fatigue crack growth in aluminum-lithium alloys, in: "Proceedings of the 3rd International Aluminium-Lithium Conference," Oxford, England, July, 1985, Pergamon Press, in press.
12. P.E. Bretz, L.N. Mueller, and A.K. Vasudévan, Fatigue properties of 2020-T651 aluminum alloy, in: "Aluminum-Lithium Alloys II," T.H. Sanders, Jr. and E.A. Starke, Jr., eds., AIME, Warrendale, Pennsylvania (1981), 543.

Table 1. Registered Composition Limits for 2090 in Weight Percent.

| Al | Cu | Li | Zr | Fe | Si | Mg | Mn | Ti |
|---|---|---|---|---|---|---|---|---|
| bal | 2.4-3.0 | 1.9-2.6 | 0.08-0.15 | 0.10 | 0.12 | 0.25 | 0.05 | 0.15 |

Table 2. Strength, Elongation, and Fracture Toughness of 2090-T8E41 at Room, Liquid Nitrogen, and Liquid Helium Temperatures.

| Test Temperature K | Yield Strength (MPa) | | U.T.S. (MPa) | | Elongation (in 25.4 mm) (%) | | $K_{Ic}$ (MPa$\sqrt{m}$) | |
|---|---|---|---|---|---|---|---|---|
| | L | LT | L | LT | L | LT | L-T | T-L |
| 298 | 535 | 535 | 565 | 565 | 11.0 | 5.5 | 34 | 25 |
| 77 | 600 | 625 | 715 | 695 | 13.5 | 5.5 | 52 | 34 |
| 4 | 615 | 705 | 820 | 815 | 17.5 | 6.5 | 65 | 39 |

Table 3. Comparison of Cryogenic Mechanical Properties of 2090-T8E41 with 2219-T87. The 2219 data are taken from references 7 (298 K, 77 K tensile properties), 8 (298 K, 77 K fracture toughness) and 9 (4 K).

| Alloy | Yield Strength (MPa) | | | % Elongation* | | | $K_{Ic}$ (MPa$\sqrt{m}$) | | |
|---|---|---|---|---|---|---|---|---|---|
| | 298 K | 77 K | 4 K | 298 K | 77 K | 4 K | 298 K | 77 K | 4 K |
| 2090-T8E41 | 535 | 600 | 615 | 11.0 | 13.5 | 17.5 | 34 | 52 | 65 |
| 2219-T87 | 386 | 461 | 512 | 11.8 | 14.0 | - | 36 | 43 | 48 |

* 2090: elongation in 25.4mm (1.0in); 2219: elongation in 50.8mm (2.0in)

REFERENCES

1. W.E. Quist, G.H. Narayanan and A.L. Wingert, in: Aluminum-Lithium Alloys II, T.H. Sanders, Jr. and E.A. Starke, Jr., eds., AIME, Warrendale, PA (1981), 313.

2. R.R. Sawtell, P.E. Bretz, J.I. Petit and A.K. Vasudevan, in: Proceedings of 1984 SAE/Aerospace Congress and Exposition, Long Beach, CA, Oct. 15-18, 1984, in press.

3. D. Webster, Met. Prog. 125:33 (1984).

4. D. Webster, Proceedings of the 3rd International Aluminium-Lithium Conference, Oxford, England, July, 1985, Pergamon Press, in press.

5. R.J. Rioja and E.A. Ludwiczak, 3rd International Aluminium-Lithium Conference, Oxford, England, July, 1985, Pergamon Press, in press.

6. J.G. Kaufman and E.W. Johnson, in: "Advances in Cryogenic Engineering," vol. 6, Plenum Press, New York, (1960), 637.

7. J.G. Kaufman, F.G. Nelson, and E.W. Johnson, in: "Advances in Cryogenic Engineering," vol. 8, Plenum Press, New York, (1963) 661.

8. J.G. Kaufman and M. Holt, in: "Advances in Cryogenic Engineering," vol. 10, Plenum Press, New York (1965), 77.

9. C. Fiftal, NBS/DOE report on Cryogenic Structural Materials for Superconducting Magnets, Vol. 1, 1978.

10. W. Yu, PhD thesis, University of Minnesota, 1983.

11. S. Suresh and A.K. Vasudevan, in: "Proceedings of the 3rd International Aluminium-Lithium Conference," Oxford, England, July, 1985, Pergamon Press, in press.

12. P.E. Bretz, L.N. Mueller, and A.K. Vasudevan, in: Aluminum-Lithium Alloys II, T.H. Sanders, Jr. and E.A. Starke, Jr., eds., AIME, Warrendale, PA (1981), 543.

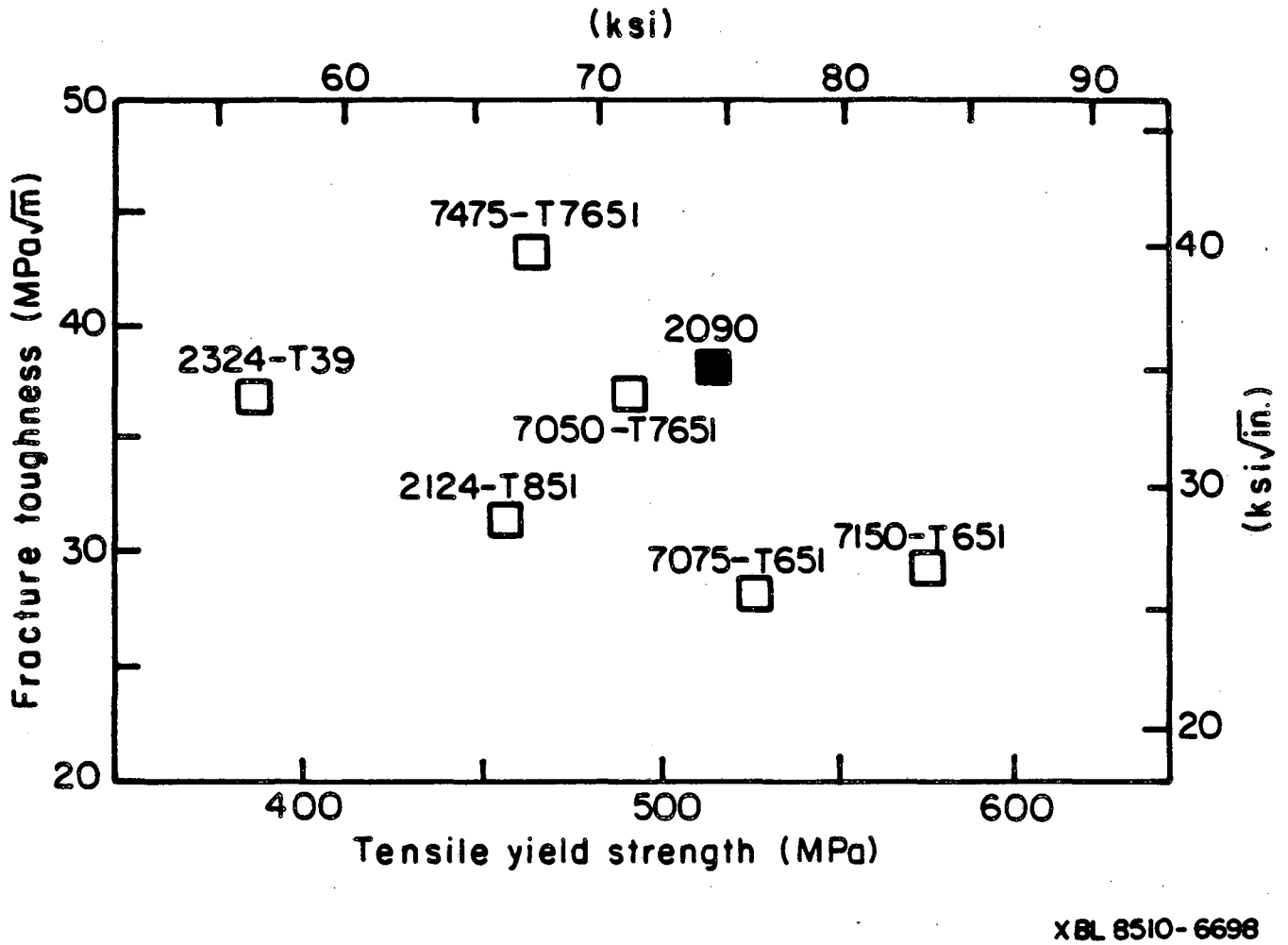


Fig. 1. Comparison of the longitudinal properties in plate material of alloy 2090-T8 to standard aerospace aluminum alloys.

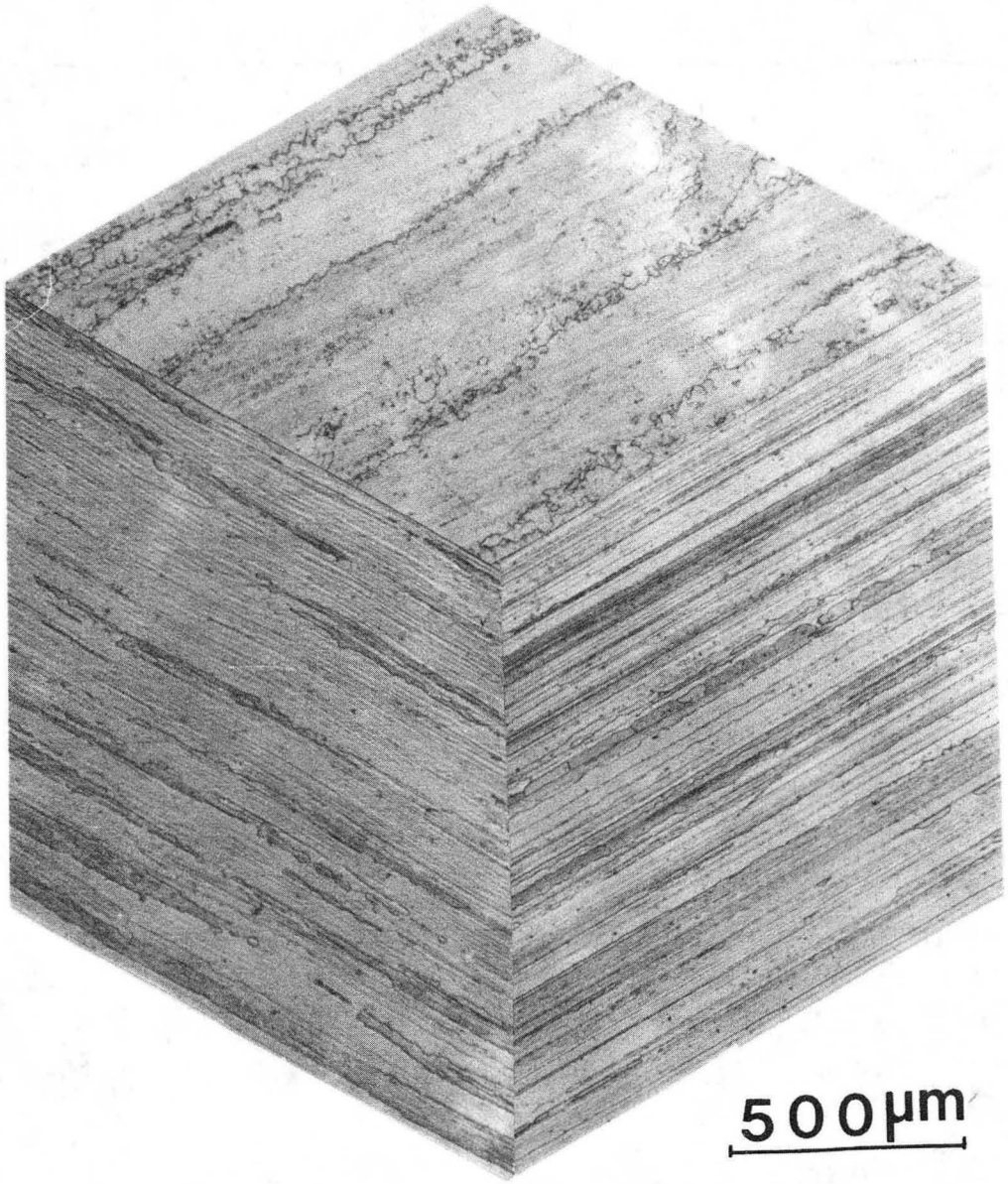


XBB 857-5875

Fig. 2. Grain structure of 12.7 mm (0.5 in) plate of 2090.

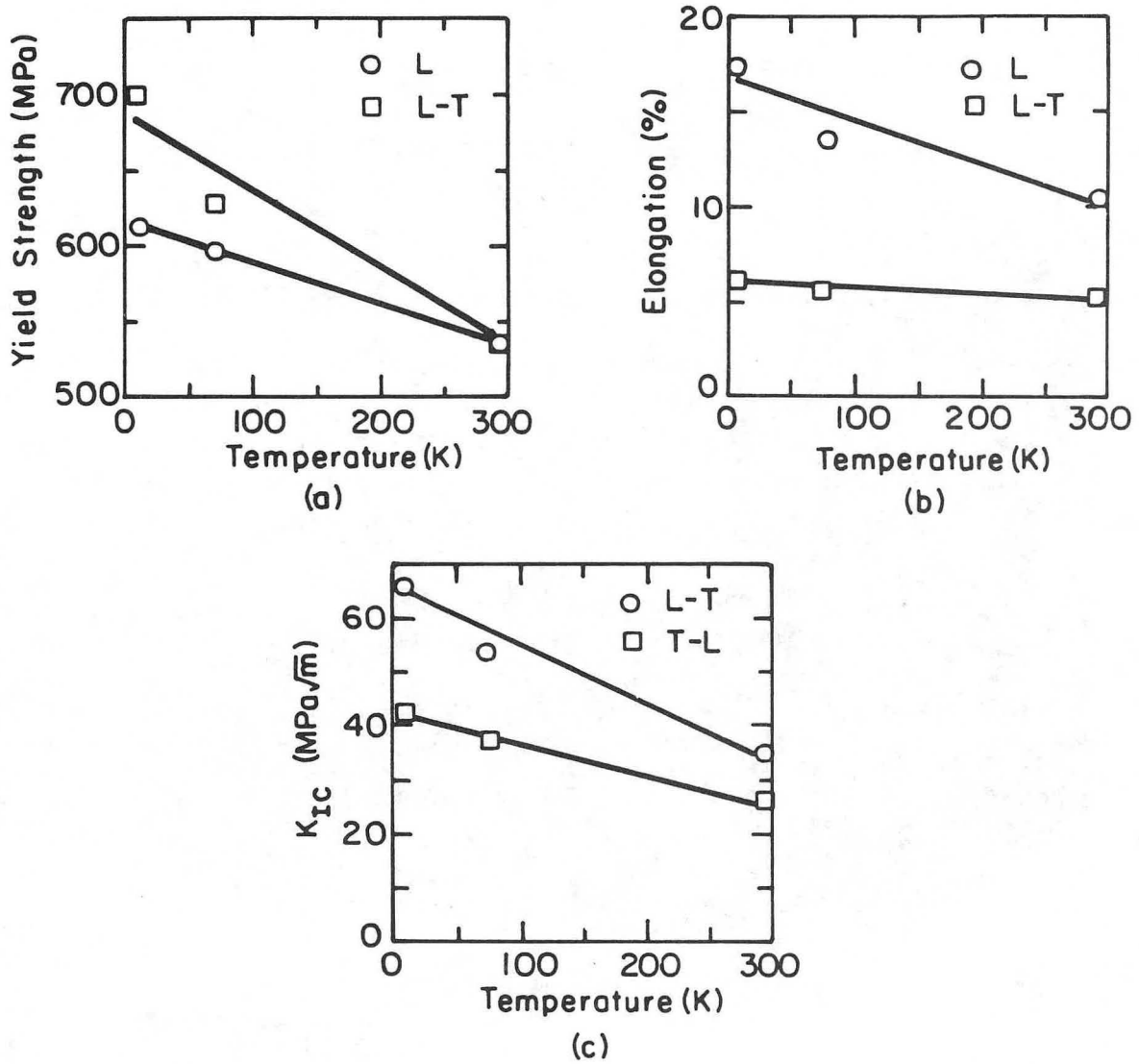


XBL858-6544

Fig. 3. Mechanical properties of 2090-T8E41 as a function of temperature.

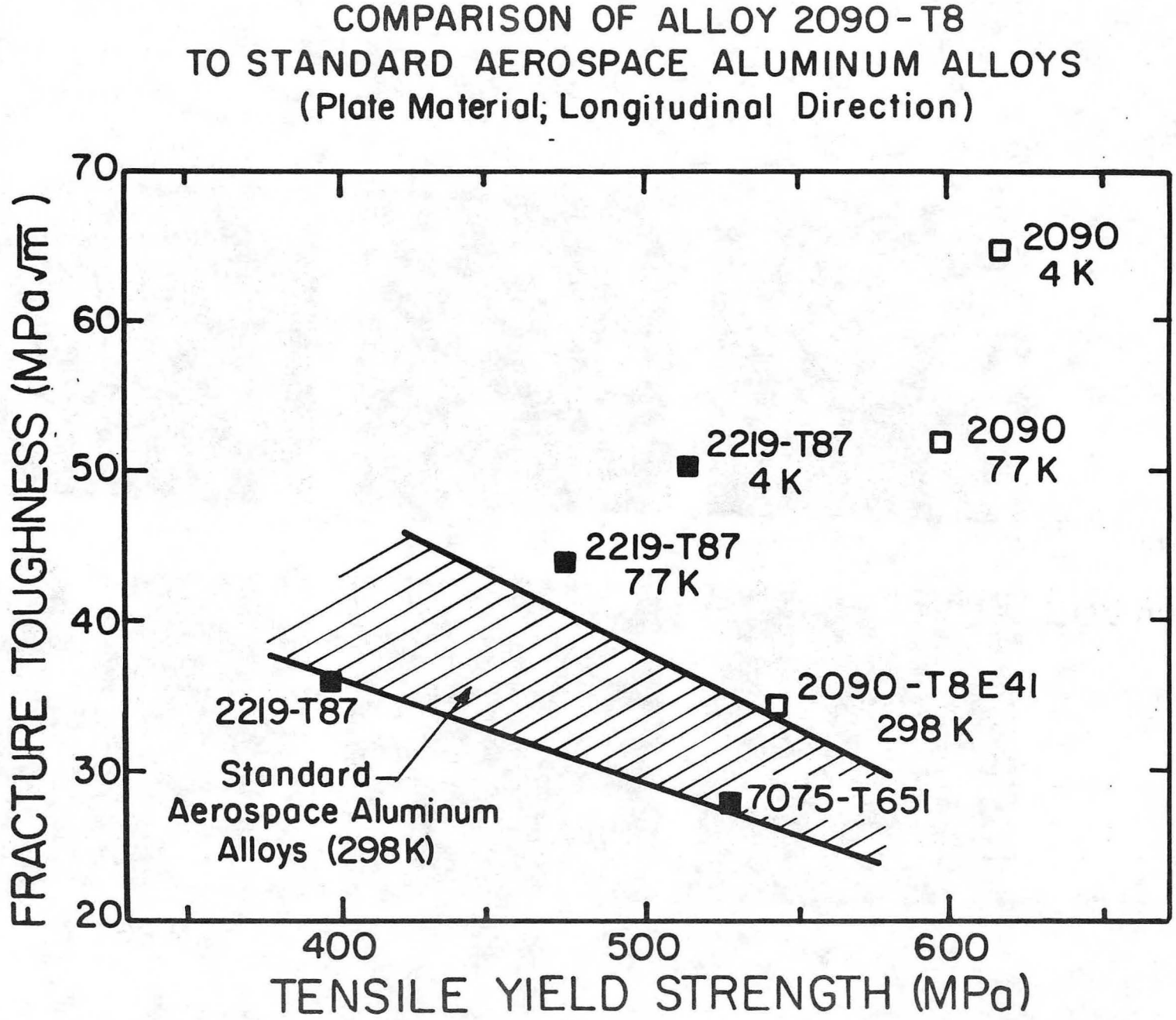


Fig. 4. Comparison of longitudinal cryogenic properties of 2090-T8E41 to standard aerospace alloys.

XBL 858-6543 A

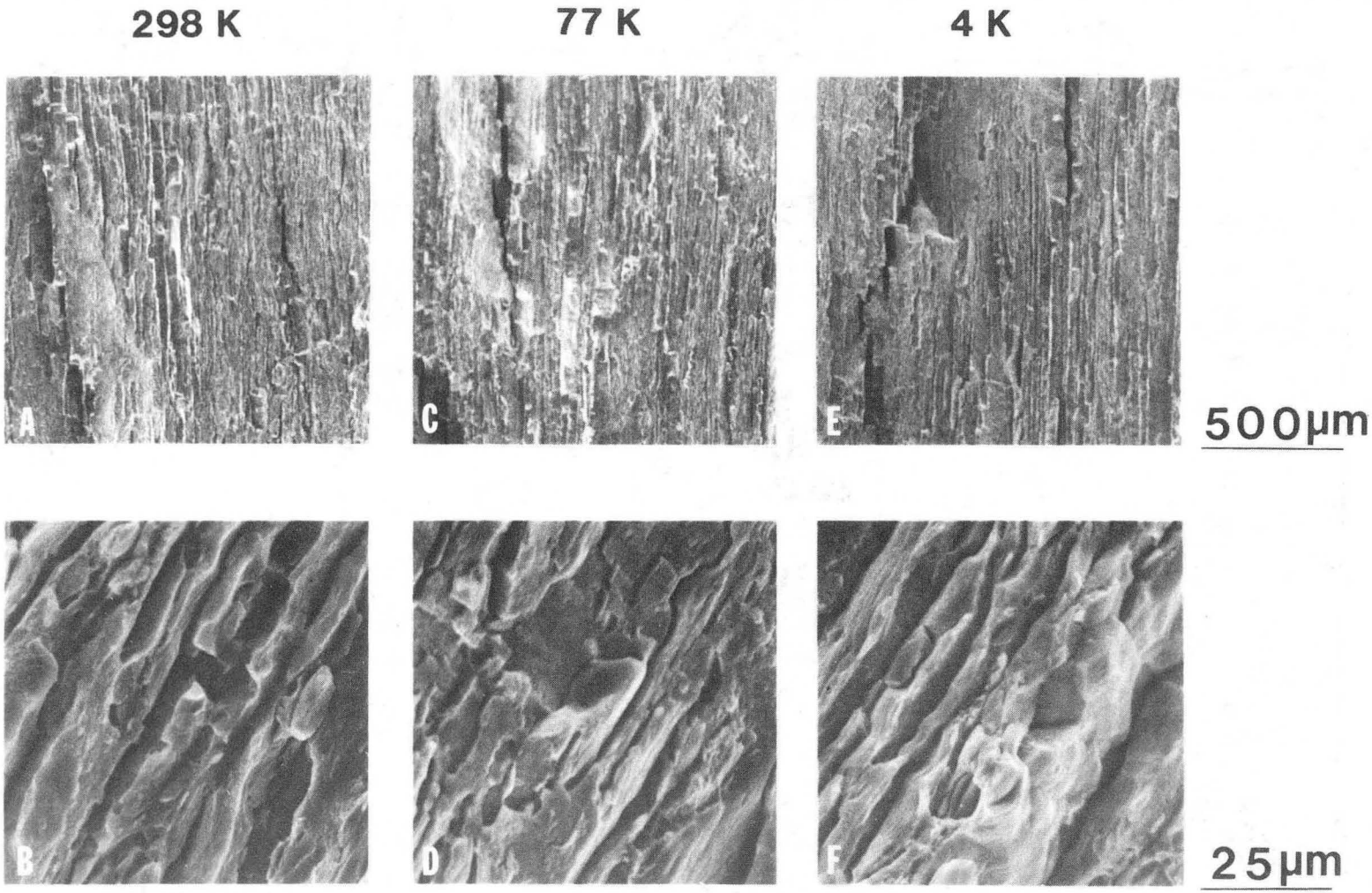


KBB 858-5979

Fig. 5. Comparison of fracture surfaces of $J_{Ic}$ specimens in the L-T orientation broken at a),b) 298 K, c),d) 77 K and e),f) 4 K.

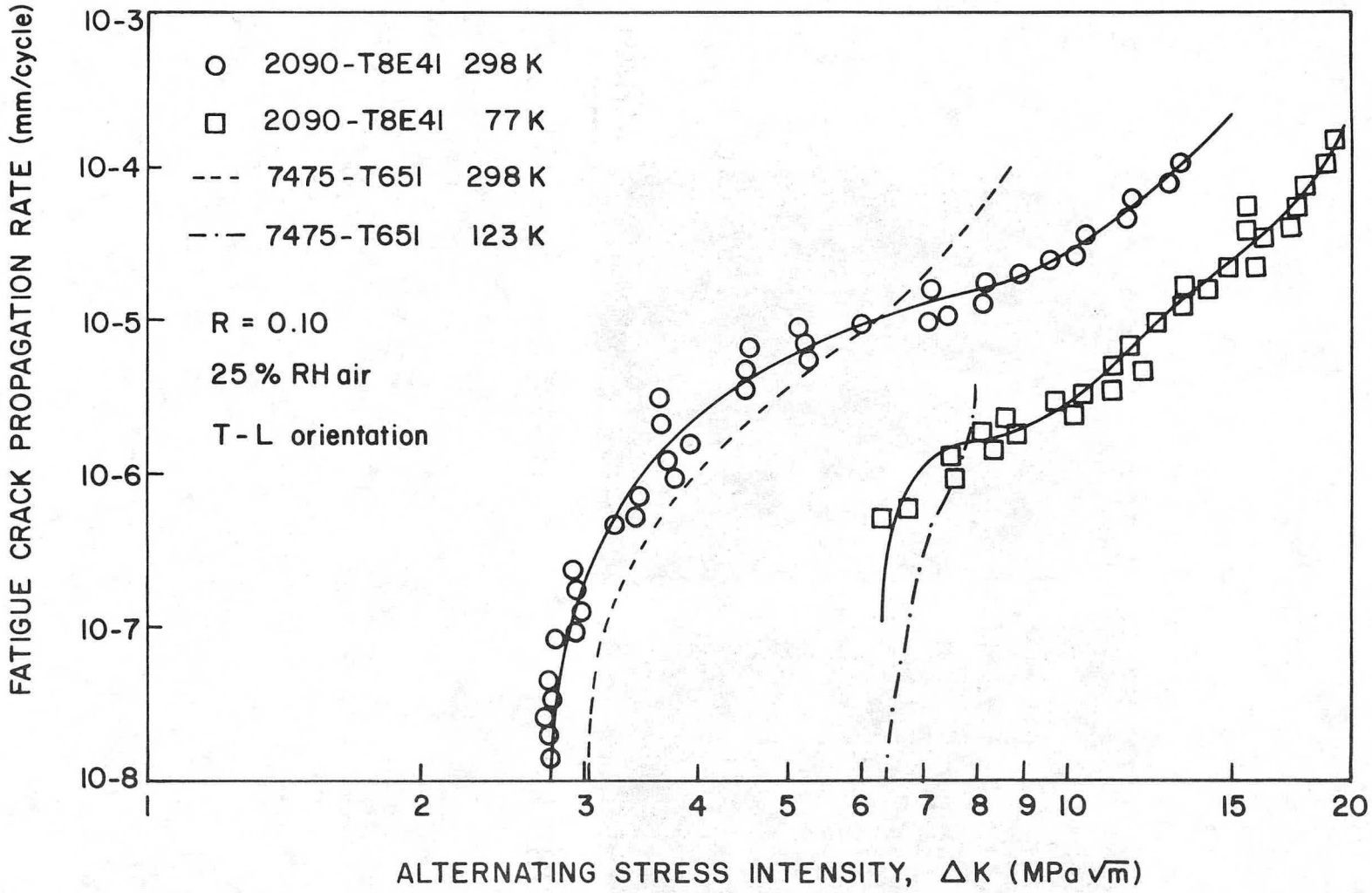


XBL 858-3415

Fig. 6. Effect of temperature on the fatigue crack propagation rates in 2090-T8 and 7475-T651.

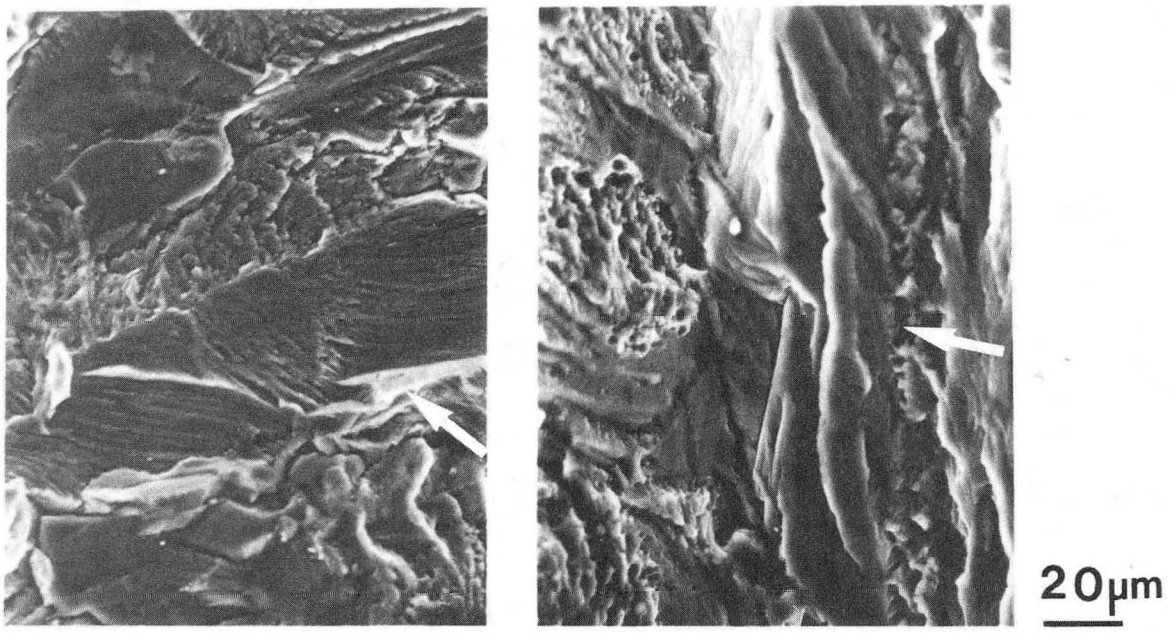


Fig. 7. Comparison of fatigue crack surface appearance in the near-threshold region of specimens. a) $\Delta K$ = 2.6 MPa$\sqrt{m}$ at 298 K, and b) $\Delta K$ = 6.3 MPa$\sqrt{m}$ at 77 K. Arrow indicates general direction of crack growth.

*LAWRENCE BERKELEY LABORATORY*
*TECHNICAL INFORMATION DEPARTMENT*
*UNIVERSITY OF CALIFORNIA*
*BERKELEY, CALIFORNIA 94720*